Technical Note	LIGO-T2200172-v3	2022/10/06

Actively Monitoring and Increasing Stability of the Auxiliary Laser Controls

Cici Hanna

Contents

Abstract

Auxiliary (AUX) lasers in the Laser Interferometer Gravitational-wave Observatory (LIGO) interferometers are at the core of the arm length stabilization (ALS) system. This system is routinely used to lock the interferometer to its nominal operating point for gravitational wave (GW) detection. Furthermore, the possibility of using the AUX laser system as a future calibration scheme has been suggested. In order to better understand the viability of an AUX laser calibration scheme, measuring the systematics of the AUX laser control loop is necessary. I used a Red Pitaya as a small and inexpensive measurement device to measure the Unity Gain Frequency of the AUX control loop, in order to easily monitor the gain of the AUX controls over long periods of time. I also developed an inversion filter to cancel out the resonances of the AUX control loop actuator, in order to increase overall loop stability.

1 Introduction

1.1 Overview of the AUX Laser

Tiny ripples in the fabric of spacetime from a pair of coalescing black holes were first detected by the LIGO observatories in 2015 [2]. The sensitivity in ground-based detectors such as aLIGO stems from its 4km long Michelson interferometer with Fabry-Perot (FP) cavities along its arms. Together with the effect of 'power' and 'signal' recycling cavities, the interferometer is sensitive to differential arm motion from gravitationally induced strain in the order of a part in 10^{-23} in the audio band from 10 - 1000 Hz. In order for the LIGO interferometer to reach its ultimate sensitivity it must be "locked", which means that the frequency of the main laser or "pre-stabilized laser" (PSL) must be fixed to five coupled degrees of freedom. The process of locking a single degree of freedom is as follows: when the PSL is incident on a cavity (for example, the X arm cavity), the Pound–Drever–Hall (PDH) technique measures the difference between the resonance of the cavity and the PSL frequency [4] using the reflected light. Although the laser frequency fluctuates due to random environmental changes, at frequencies above ~ 10 Hz, the PSL free-running noise is less than that of the residual arm motion, so appropriate feedback control can adjust the cavity mirror to bring keep the laser frequency resonant. Thus we constrain, or "lock", the cavity length to the frequency of the PSL.

Locking one cavity to the PSL is a relatively simple controls problem. Locking two *coupled* cavities at once can be more complicated. Locking all five degrees of freedom that must be controlled in the LIGO interferometer—the two cavities, the power recycling cavity, the signal recycling cavity, and the Michelson degree of freedom—becomes increasingly complicated. In order to simplify this task, we use Auxiliary (AUX) lasers to independently probe arm cavities, as illustrated in Fig. 1.

The AUX lasers of the LIGO interferometer make the lock acquisition process more deterministic and robust. There are two AUX lasers, one for each arm cavity, but both function
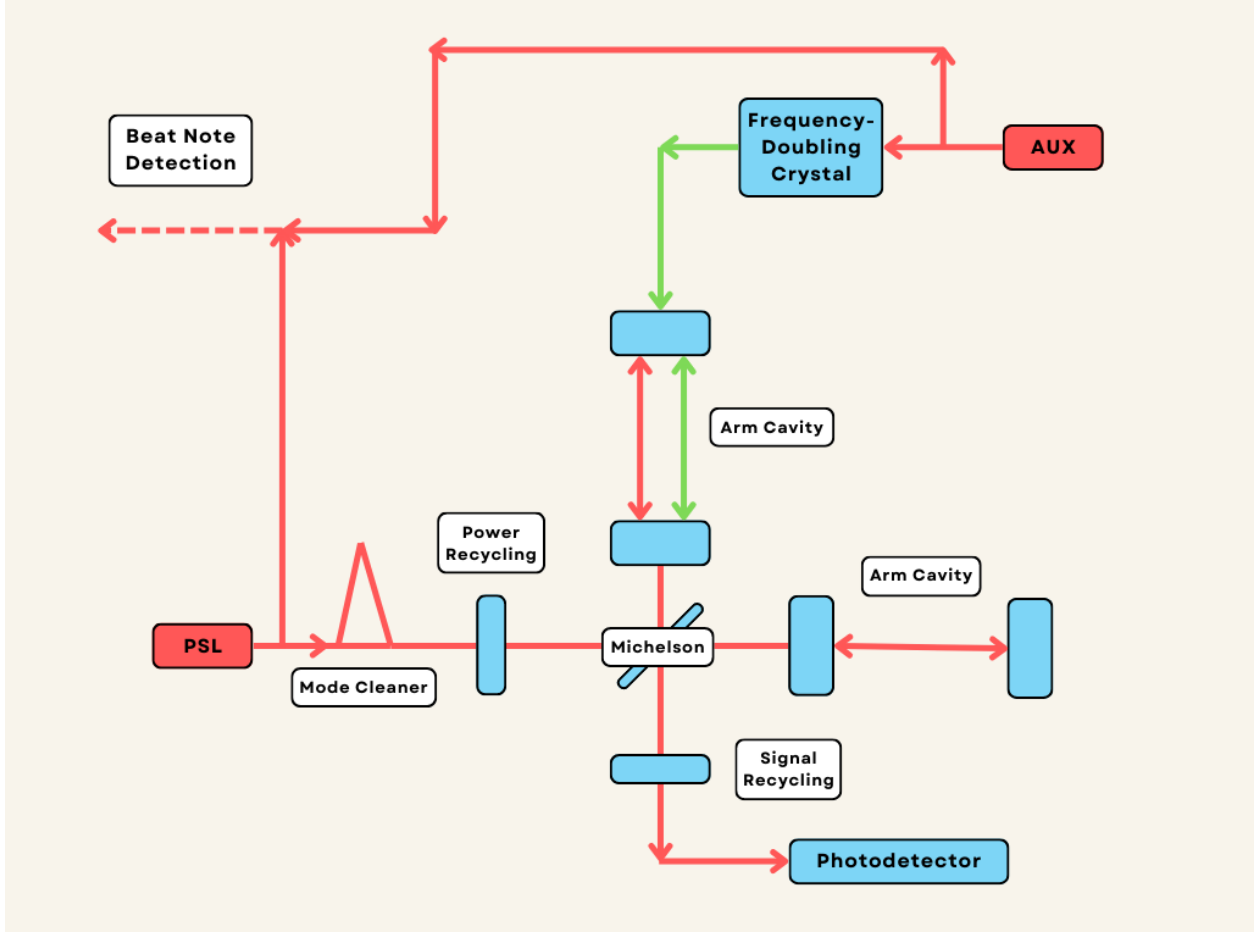
Figure 1: Schematic diagram of the interferometer showing the PSL, main sections of the interferometer, and AUX laser for one arm cavity. For ALS, the beatnote is taken by interfering both laser beams in a fast photodetector (not shown).

the same way. The AUX laser seed is the same kind as the PSL—an Nd:YAG nonplanar ring oscillator (NPRO) laser centered at 1064 nm—but a fraction of it is frequency-doubled by a nonlinear crystal before entering the arm cavity. The test masses are coated to reflect both green and infrared light, but the other optics in the interferometer—the power recycling mirror, etc.—are only coated to reflect infrared light. Thus the 532 nm frequency doubled AUX laser entering the interferometer only interacts with the arm cavity. In order to extract the information about the cavity length without locking the cavity to the PSL, we lock the AUX laser to the cavity. We use the same PDH technique detailed above, but instead of adjusting the cavity mirrors to keep the cavity length locked to the AUX frequency, we adjust the AUX frequency to bring the laser into resonance. We do this by adjusting the voltage applied to a piezo-electric transducer (PZT) straining the Nd:YAG crystal inside the laser. Finally, each AUX laser is compared to the PSL by beating them in a fast photodetector, as shown in Fig. 1. Since each AUX laser is locked to an arm cavity, we can see how far off the PSL is from the X- and Y-arm cavity resonances before we lock each arm cavity to the PSL. This is helpful for lock acquisition of the whole interferometer since knowing how far the PSL is from the coupled cavity resonances allows us to keep the degrees of freedom

away or close from resonance as we stabilize other components. [7, 8].

1.2   Proposed Future Calibration Scheme

The Photon calibrator (PCal) [5] operates by shooting a beam of photons at a test mass and calculating how much each photon should move the test mass, to find the differential arm length as illustrated in Fig. 2. However, even though the number of photons exiting the transmitter module can be known, less photons are generally incident on the receiver module due to various losses. Thus the number of photons that hit the test mass cannot be known with arbitrary precision, giving the roughly 2% uncertainty of the current calibration scheme. The second largest contribution to this uncertainty comes from calculating the test mass movement, since the differential arm length cannot be measured directly.
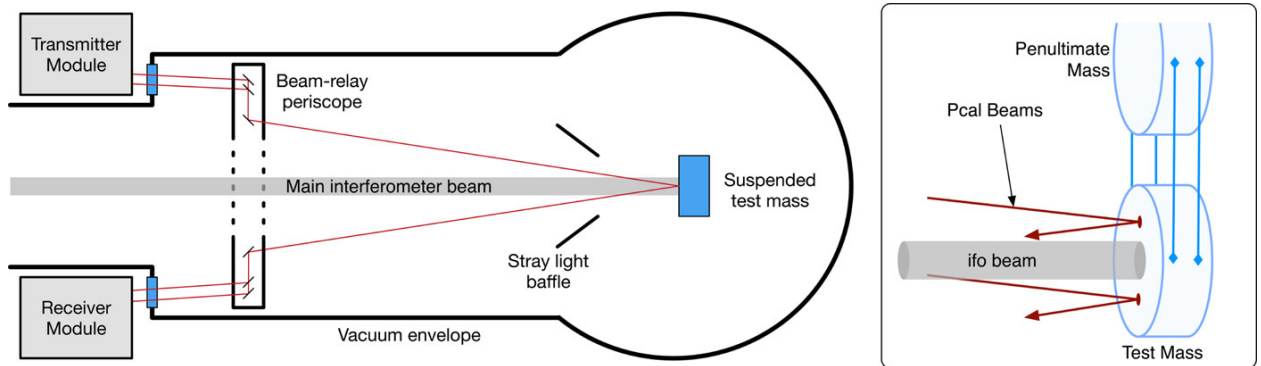

Figure 2: The current Pcal calibration scheme. Photons leave the transmitter module, hit the test mass as shown, and then are measured on the receiver module [5].

The PCal calibration scheme is effective and precise enough for LIGO to do extensive parameter estimation analysis on detected gravitational waves. At Caltech's 40m Lab a new calibration scheme using the AUX laser system is being prototyped. This new calibration method uses the beat note of the PSL and one AUX laser to measure differential arm length directly (see Fig. 3). Thus we can compare a direct measurement of differential arm length to light intensity exiting the interferometer, instead of a calculated value. This measurement is also frequency-based instead of based on photon incidence, which could allow a higher degree of precision. The goal is to reach a 0.1% level calibration under similar signal-to-noise (SNR) ratio conditions. More precise detector calibration would allow us to reduce uncertainties on astrophysical parameter estimation.

2   Methods
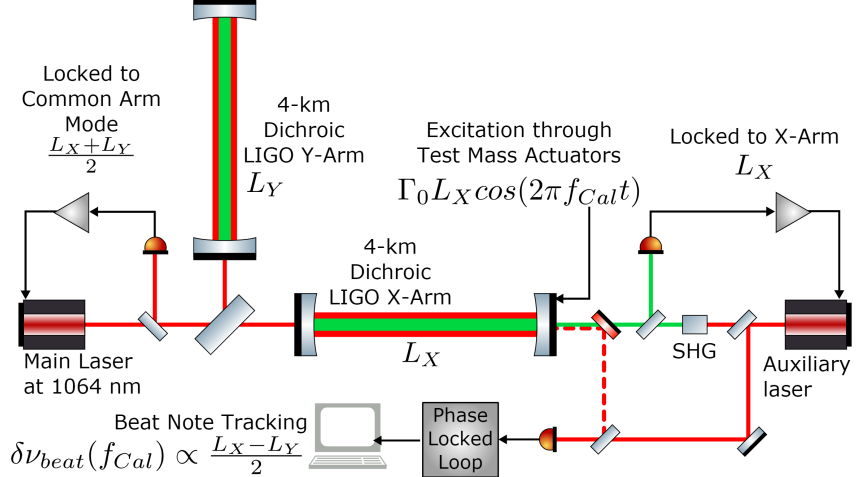
Figure 3: The proposed AUX laser calibration scheme. Since the frequency of the PSL is proportional to the common arm mode, taking the beat note with one arm (as shown, the X-arm) yields a beat note frequency proportional to the differential arm length. Thus obtain a direct, frequency-based measurement of differential arm length that can be used for calibration [6].

2.1 AUX Laser Control Loop

The control loop of the AUX laser consists of four main components (see Fig. 4). The PZT actuator inside the laser changes the frequency of the laser comprising the plant in our loop. The PDH discriminator determines how far off the laser frequency is from the nearest cavity resonance. The PDH error signal passes through a servo producing an appropriate correcting voltage for the actuator. Various noise sources enter at different places in the loop as shown in Fig. 4, including the free-running noise of the AUX laser (α) and actuator noise (ϵ).

Multiplying the transfer functions of each of the components yields the Open Loop Gain (OLG) of the loop ($G_{OL}(f) = KACD$), which describes the gain of a signal that goes around the loop once as a function of frequency. However, since the control system is a closed loop, a signal that enters the loop does not go around once, but continues to circle the loop until either it is effectively suppressed or it amplifies to a point that the laser loses lock and the loop opens. The Closed Loop Gain ($G_{CL}(f)$) describes the asymptotic long-term behavior of a signal that enters the loop and circles around continuously. The Closed Loop Gain is found by taking

$$G_{CL}(f) = \frac{1}{1 - G_{OL}(f)} \tag{1}$$

It is clear from Equation 1 that the frequency at which $G_{OL} = 1$ is of importance. Past this frequency called the Unity Gain Frequency (UGF), our control loop is unable to minimize signals and begins to loop back upon itself, amplifying noises instead of suppressing them.
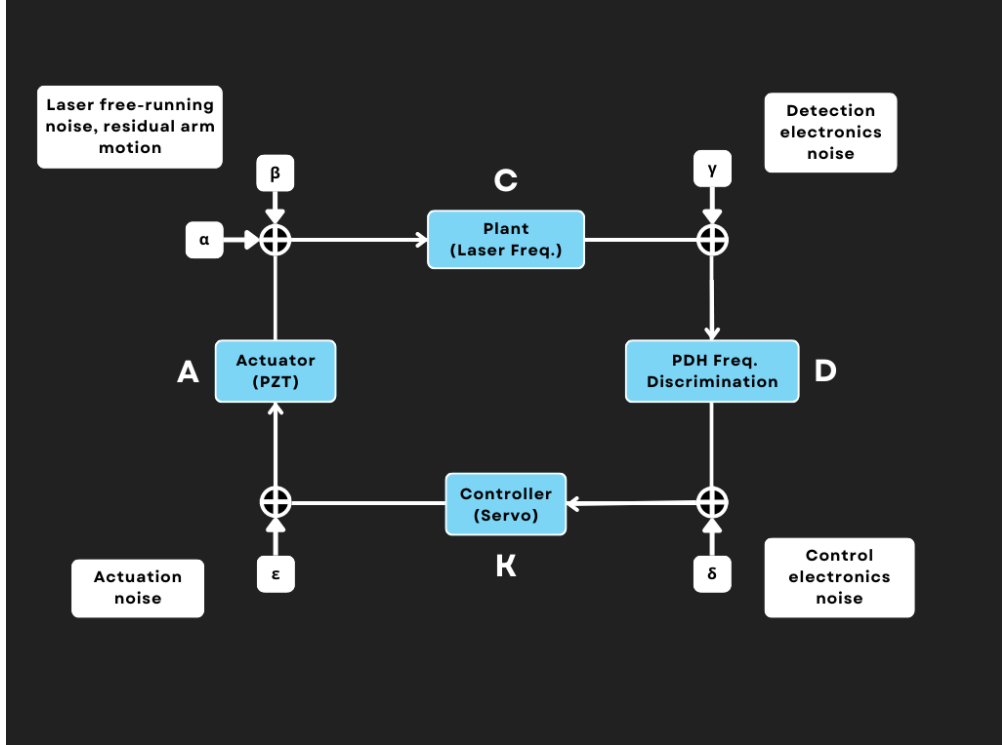
Figure 4: The main features of the AUX laser control loop.

Thus, the UGF is a simple metric for the functional frequency range of our control loop, and how that range changes over time. Monitoring the UGF of the AUX control system allows us a to examine systematic effects on the gain of the controls, and thus better understand the limitations of using the AUX laser system for calibration.

2.2 RedPitaya UGF Monitoring System

In order to monitor the UGF changing over time, I used a Red Pitaya STEMLab 125-10. The Red Pitaya is a multifunctional FPGA that I used as a vector network analyzer (VNA) to measure the OLG of the AUX laser control loop as depicted by Fig. 5. I wrote a Python script using the Red Pitaya SCPI interface [1] to send in a swept sine of a given frequency range and measure the transfer function of the OLG along with the coherence. The code takes each frequency in the range, sends it into the control loop in Fig. 5, measures the outputs at two points in the loop, and divides output 2 by output 1 to find the transfer function of the OLG at that frequency. Additionally, `scipy.signal.coherence` calculates the coherence at that frequency. The code then repeats the process for each frequency in the range to create a swept sine input and get a transfer function with coherence over the desired frequency band. I approximated the region of the transfer function H surrounding the UGF as linear (on a log-log scale), and found the UGF and corresponding phase margin as illustrated in Fig. 6. I propagated my measurement statistical uncertainty using Bendat and Piersol's textbook "Random Data: Analysis and Measurement Procedures" [3], which approximates fractional uncertainty in $|H|$ and $\angle H$ as:
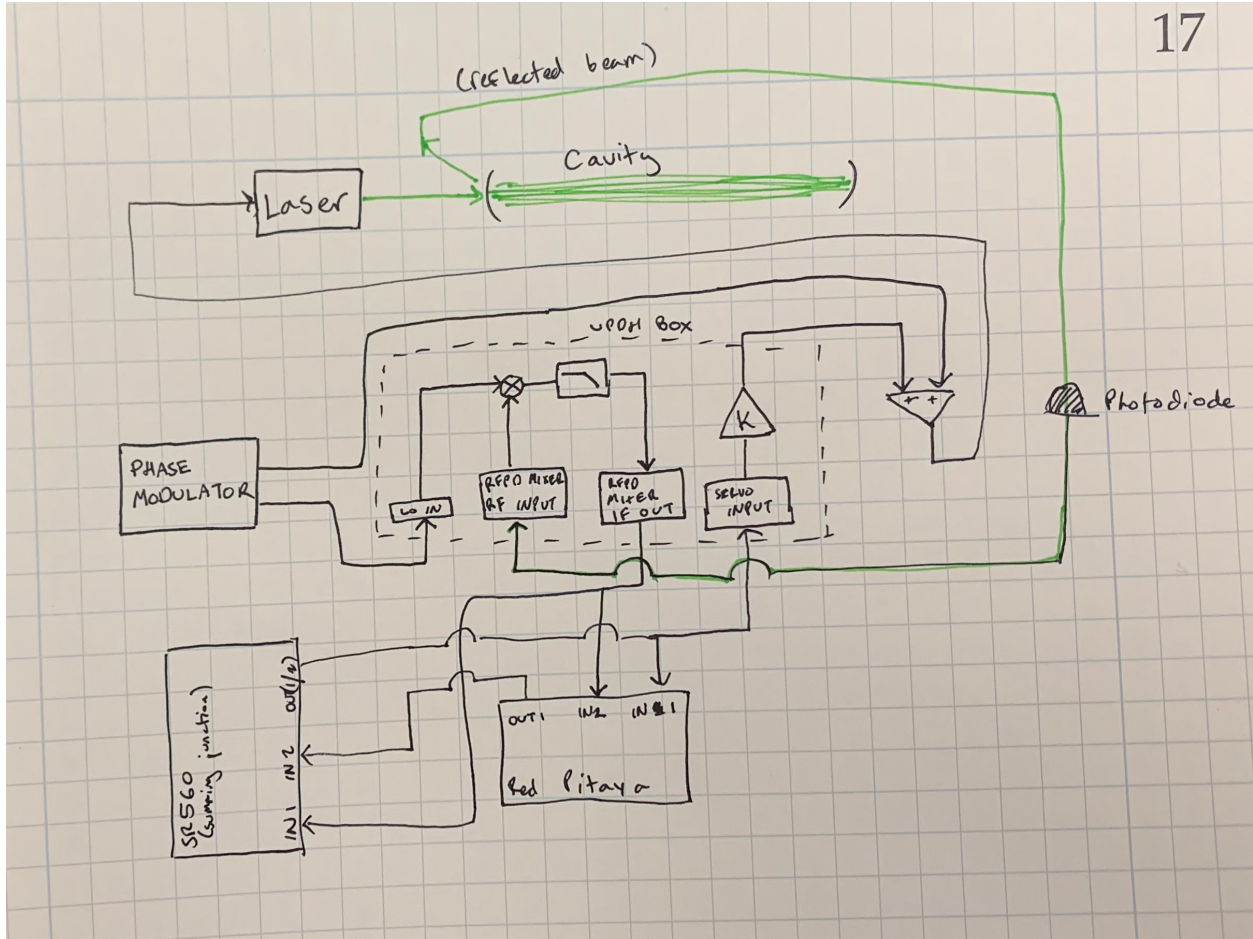
Figure 5:   Diagram of the Red Pitaya VNA for the AUX laser control loop. Instead of measuring or self-referencing the swept sine that it inserts into the loop, the Red Pitaya takes as input two points within the loop, so that it measures the transfer function of the OLG directly.

$$\Delta\,|H| = \Delta\angle H = \frac{(1 - \gamma^2(f))^{1/2}}{|\gamma(f)|\,\sqrt{2n}} \tag{2}$$

where $\gamma(f)$ is the coherence at each frequency and n is the number of averages. For the data shown in Fig. 6, $n = 1$.

There are multiple advantages of a Red Pitaya monitoring VNA over a larger, high-precision VNA such as the SR785 Dynamic Signal Analyzer. The Red Pitaya is much smaller, whereas a large VNA must be set up on a cart. A Red Pitaya can be permanently installed near the AUX controls to measure the loop for weeks or months without taking up much space. A Red Pitaya is also far less expensive than an SR785 or comparable device, and therefore a lab can afford to leave a Red Pitaya to monitor AUX control loop without needing to remove it for more important purposes whenever a VNA is required. The disadvantages of the Red Pitaya include a limited frequency range and a lower SNR than a more precise analog measurement

OLTF - X-Arm AUX Laser Lock

UGF = 13.4 ± 1.2 kHz
PM = 63.3 ± 5.3°
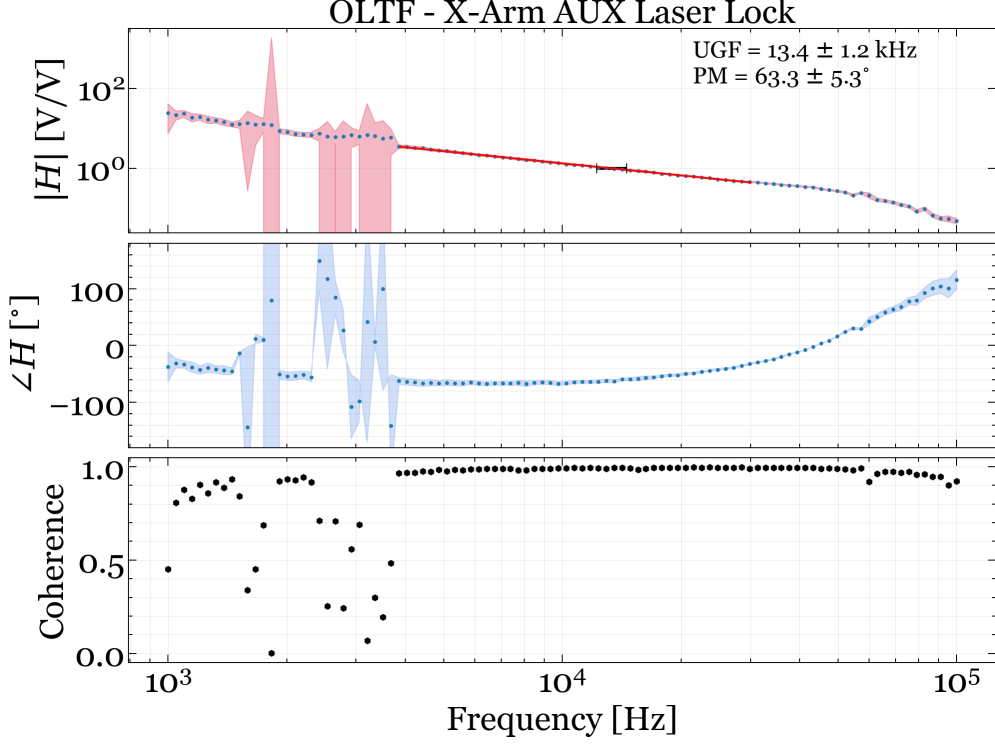
Figure 6: Example OLG of the AUX control loop. A linear fit of the region surrounding the UGF yields an estimate of the UGF and phase margin. Uncertainty is propagated as a function of coherence.

device like an SR785 due to ADC/DAC noise. We also could not readily deploy the device on the local network because it requires wired access. However, the frequency range of the Red Pitaya includes the likely UGF values of the AUX loop, and being able to monitor how the UGF changes over time is easier with low-precision but frequent measurements than it would be with high-precision but infrequent measurements.

We verified a known systematic effect on the UGF (and thus the overall gain of the system); the optical gain of the cavity—when the laser is locked and well-aligned, the UGF tended to fall in the range of 13-17 kHz, but when the laser was locked but more poorly aligned, with a lower optical gain, the UGF tended to fall in the range of 3-6 kHz. It might be interesting to correlate this systematic with other signals in the interferometerI did not have time to quantify this effect so further measurement of UGF vs. cavity optical gain would be of interest.

2.3 Damping of the AUX Laser Actuator Resonances

The AUX control loop suppresses laser frequency noise up to the UGF of ~ 13 kHz, so extending its bandwidth would allow increased gain to further suppress high frequency noise. In order to increase the gain of AUX laser control loop, I also worked on creating a digital filter to invert the resonances of the PZT inside the laser. At frequencies above 100 kHz,

the resonant modes of the PZT itself become apparent, adding significant phase lag and decreasing the loop gain. In order to improve loop stability at high frequencies, we first measure the actuator (PZT) transfer function at high frequencies using a Liquid Instruments Moku:Pro instead of the Red Pitaya, since the Moku could handle higher frequencies with higher precision, and because it has the ability to implement digital filters to cancel out the resonances

We measured the AUX PZT transfer function by the swept sine method described above, and tracked the demodulated PSL-AUX beatnote using a delay-line frequency discriminator (DFD). The 10 m DFD tracks frequency fluctuations in the beatnote and translates them into an output voltage with magnitude.

$$V(f) = K_\phi 2\pi\tau \frac{\sin(\pi f \tau)}{\pi f \tau} \tag{3}$$

where $\tau \simeq 44$ns is the delay time equal to the delay line length divided by the speed of light within the cable ($0.75c$, with $c \simeq 3 \times 10^8$ m/s the speed of light), $K_\phi \simeq 1$V/rad. Because our measurement takes place at frequencies $f < \tau^{-1}$, our DFD calibration is approximately constant and equal to 0.044μV/Hz.

Using a manual fit (selecting and tuning poles and zeros visually) with 5 pairs of zeros and 5 pairs of poles, I fit the calibrated TF data and inverted the fit, as shown in Fig. 7.
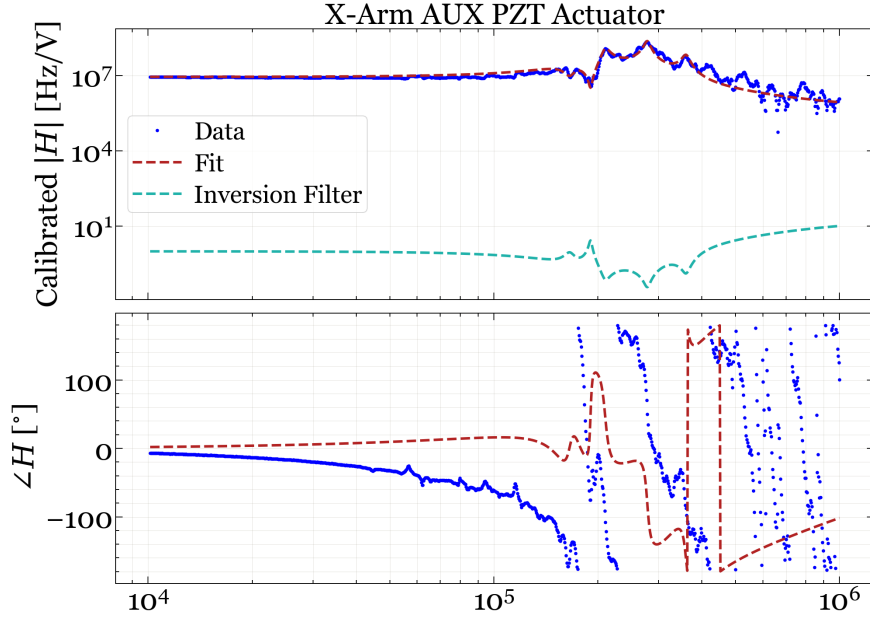
Figure 7: Measured actuator transfer function (ATF), calibrated with the transfer function of the DFD. A manual fit over the data, using five pole pairs and five zero pairs, and (shown for magnitude only) the inversion of the fit.

With the best fit parameters found above, I spliced in the measured data from 10 kHz to 1 MHz into a prediction of the actuator transfer function and used it to model the OLG by multiplying with models of the transfer functions of the other components of the loop. I

then multiplied in the transfer function of my inverted fit of the AUX PZT, to simulate the effects of adding a digital cancellation filter. This is shown in Fig. 8. As cam be seen in the phase of Fig. 8, the "bubble" visible from 1-50 kHz shifts to the right to   2-100 kHz. The shift in this phase means that the phase margin of the UGF will prevent it from reaching $1 + 0i$, which would cause the loop to lose stability. Thus, this inversion filter would increase the stability of the AUX laser control loop, and implementing it will increase the range of stable frequencies at which the loop can suppress noise.
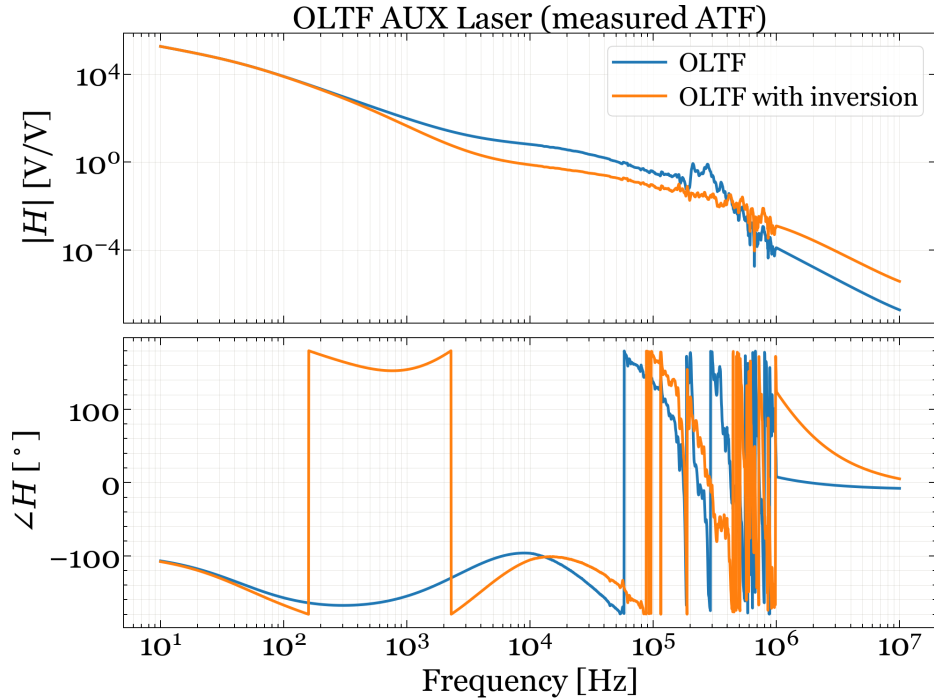
Figure 8: Open loop transfer function (OLTF) of the AUX laser, without and with the inversion filter applied.

3 Ongoing Work

3.1 Damping of Actuator Resonances

Implementing the inversion filter described in Section 2.3 would improve loop stability. The Moku:Pro can be used to create digital filters, and could be pursued as a way to implement inversion of the PZT resonances. Refinement of the inversion filter is also an area for future development—the current fit is a simple manual fit based on visual estimation of the poles and zeros, but using a function such as vector fitting could increase the accuracy of the fit and effectiveness of the inversion filter.

3.2 Refining Proposed Control Scheme

Future work on the proposed AUX laser control scheme includes a more thorough and quantitative examination of effects on control loop gain (such as cavity optical gain).

4 Acknowledgements

I would like to thank my mentors, Dr. Francisco Salces-Carcoba, Anchal Gupta, and Dr. Rana Adhikari, for their continuous guidance, support, and encouragement. Thank you also to Alan J. Weinstein and all the LIGO mentors for this excellent program, as well as the LIGO Collaboration and the NSF.

References

[1] RedPitaya scpi server. https://redpitaya.readthedocs.io/en/latest/appsFeatures/remoteControl/remoteControl.html. Accessed: 2022-08-06.

[2] B. P. Abbott, R. Abbott, T. D. Abbott, M. R. Abernathy, F. Acernese, K. Ackley, C. Adams, T. Adams, P. Addesso, R. X. Adhikari, V. B. Adya, C. Affeldt, M. Agathos, K. Agatsuma, N. Aggarwal, O. D. Aguiar, L. Aiello, A. Ain, P. Ajith, B. Allen, A. Allocca, P. A. Altin, S. B. Anderson, W. G. Anderson, K. Arai, M. A. Arain, M. C. Araya, C. C. Arceneaux, J. S. Areeda, N. Arnaud, K. G. Arun, S. Ascenzi, G. Ashton, M. Ast, S. M. Aston, P. Astone, P. Aufmuth, C. Aulbert, S. Babak, P. Bacon, M. K. M. Bader, P. T. Baker, F. Baldaccini, G. Ballardin, S. W. Ballmer, J. C. Barayoga, S. E. Barclay, B. C. Barish, D. Barker, F. Barone, B. Barr, L. Barsotti, M. Barsuglia, D. Barta, J. Bartlett, M. A. Barton, I. Bartos, R. Bassiri, A. Basti, J. C. Batch, C. Baune, V. Bavigadda, M. Bazzan, B. Behnke, M. Bejger, C. Belczynski, A. S. Bell, C. J. Bell, B. K. Berger, J. Bergman, G. Bergmann, C. P. L. Berry, D. Bersanetti, A. Bertolini, J. Betzwieser, S. Bhagwat, R. Bhandare, I. A. Bilenko, G. Billingsley, J. Birch, R. Birney, O. Birnholtz, S. Biscans, A. Bisht, M. Bitossi, C. Biwer, M. A. Bizouard, J. K. Blackburn, C. D. Blair, D. G. Blair, R. M. Blair, S. Bloemen, O. Bock, T. P. Bodiya, M. Boer, G. Bogaert, C. Bogan, A. Bohe, P. Bojtos, C. Bond, F. Bondu, R. Bonnand, B. A. Boom, R. Bork, V. Boschi, S. Bose, Y. Bouffanais, A. Bozzi, C. Bradaschia, P. R. Brady, V. B. Braginsky, M. Branchesi, J. E. Brau, T. Briant, A. Brillet, M. Brinkmann, V. Brisson, P. Brockill, A. F. Brooks, D. A. Brown, D. D. Brown, N. M. Brown, C. C. Buchanan, A. Buikema, T. Bulik, H. J. Bulten, A. Buonanno, D. Buskulic, C. Buy, R. L. Byer, M. Cabero, L. Cadonati, G. Cagnoli, C. Cahillane, J. Calderón Bustillo, T. Callister, E. Calloni, J. B. Camp, K. C. Cannon, J. Cao, C. D. Capano, E. Capocasa, F. Carbognani, S. Caride, J. Casanueva Diaz, C. Casentini, S. Caudill, M. Cavaglià, F. Cavalier, R. Cavalieri, G. Cella, C. B. Cepeda, L. Cerboni Baiardi, G. Cerretani, E. Cesarini, R. Chakraborty, T. Chalermsongsak, S. J. Chamberlin, M. Chan, S. Chao, P. Charlton,

E. Chassande-Mottin, H. Y. Chen, Y. Chen, C. Cheng, A. Chincarini, A. Chiummo, H. S. Cho, M. Cho, J. H. Chow, N. Christensen, Q. Chu, S. Chua, S. Chung, G. Ciani, F. Clara, J. A. Clark, F. Cleva, E. Coccia, P.-F. Cohadon, A. Colla, C. G. Collette, L. Cominsky, M. Constancio, A. Conte, L. Conti, D. Cook, T. R. Corbitt, N. Cornish, A. Corsi, S. Cortese, C. A. Costa, M. W. Coughlin, S. B. Coughlin, J.-P. Coulon, S. T. Countryman, P. Couvares, E. E. Cowan, D. M. Coward, M. J. Cowart, D. C. Coyne, R. Coyne, K. Craig, J. D. E. Creighton, T. D. Creighton, J. Cripe, S. G. Crowder, A. M. Cruise, A. Cumming, L. Cunningham, E. Cuoco, T. Dal Canton, S. L. Danilishin, S. D'Antonio, K. Danzmann, N. S. Darman, C. F. Da Silva Costa, V. Dattilo, I. Dave, H. P. Daveloza, M. Davier, G. S. Davies, E. J. Daw, R. Day, S. De, D. DeBra, G. Debreczeni, J. Degallaix, M. De Laurentis, S. Deléglise, W. Del Pozzo, T. Denker, T. Dent, H. Dereli, V. Dergachev, R. T. DeRosa, R. De Rosa, R. DeSalvo, S. Dhurandhar, M. C. Díaz, L. Di Fiore, M. Di Giovanni, A. Di Lieto, S. Di Pace, I. Di Palma, A. Di Virgilio, G. Dojcinoski, V. Dolique, F. Donovan, K. L. Dooley, S. Doravari, R. Douglas, T. P. Downes, M. Drago, R. W. P. Drever, J. C. Driggers, Z. Du, M. Ducrot, S. E. Dwyer, T. B. Edo, M. C. Edwards, A. Effler, H.-B. Eggenstein, P. Ehrens, J. Eichholz, S. S. Eikenberry, W. Engels, R. C. Essick, T. Etzel, M. Evans, T. M. Evans, R. Everett, M. Factourovich, V. Fafone, H. Fair, S. Fairhurst, X. Fan, Q. Fang, S. Farinon, B. Farr, W. M. Farr, M. Favata, M. Fays, H. Fehrmann, M. M. Fejer, D. Feldbaum, I. Ferrante, E. C. Ferreira, F. Ferrini, F. Fidecaro, L. S. Finn, I. Fiori, D. Fiorucci, R. P. Fisher, R. Flaminio, M. Fletcher, H. Fong, J.-D. Fournier, S. Franco, S. Frasca, F. Frasconi, M. Frede, Z. Frei, A. Freise, R. Frey, V. Frey, T. T. Fricke, P. Fritschel, V. V. Frolov, P. Fulda, M. Fyffe, H. A. G. Gabbard, J. R. Gair, L. Gammaitoni, S. G. Gaonkar, F. Garufi, A. Gatto, G. Gaur, N. Gehrels, G. Gemme, B. Gendre, E. Genin, A. Gennai, J. George, L. Gergely, V. Germain, Abhirup Ghosh, Archisman Ghosh, S. Ghosh, J. A. Giaime, K. D. Giardina, A. Giazotto, K. Gill, A. Glaefke, J. R. Gleason, E. Goetz, R. Goetz, L. Gondan, G. González, J. M. Gonzalez Castro, A. Gopakumar, N. A. Gordon, M. L. Gorodetsky, S. E. Gossan, M. Gosselin, R. Gouaty, C. Graef, P. B. Graff, M. Granata, A. Grant, S. Gras, C. Gray, G. Greco, A. C. Green, R. J. S. Greenhalgh, P. Groot, H. Grote, S. Grunewald, G. M. Guidi, X. Guo, A. Gupta, M. K. Gupta, K. E. Gushwa, E. K. Gustafson, R. Gustafson, J. J. Hacker, B. R. Hall, E. D. Hall, G. Hammond, M. Haney, M. M. Hanke, J. Hanks, C. Hanna, M. D. Hannam, J. Hanson, T. Hardwick, J. Harms, G. M. Harry, I. W. Harry, M. J. Hart, M. T. Hartman, C.-J. Haster, K. Haughian, J. Healy, J. Heefner, A. Heidmann, M. C. Heintze, G. Heinzel, H. Heitmann, P. Hello, G. Hemming, M. Hendry, I. S. Heng, J. Hennig, A. W. Heptonstall, M. Heurs, S. Hild, D. Hoak, K. A. Hodge, D. Hofman, S. E. Hollitt, K. Holt, D. E. Holz, P. Hopkins, D. J. Hosken, J. Hough, E. A. Houston, E. J. Howell, Y. M. Hu, S. Huang, E. A. Huerta, D. Huet, B. Hughey, S. Husa, S. H. Huttner, T. Huynh-Dinh, A. Idrisy, N. Indik, D. R. Ingram, R. Inta, H. N. Isa, J.-M. Isac, M. Isi, G. Islas, T. Isogai, B. R. Iyer, K. Izumi, M. B. Jacobson, T. Jacqmin, H. Jang, K. Jani, P. Jaranowski, S. Jawahar, F. Jiménez-Forteza, W. W. Johnson, N. K. Johnson-McDaniel, D. I. Jones, R. Jones, R. J. G. Jonker, L. Ju, K. Haris, C. V. Kalaghatgi, V. Kalogera, S. Kandhasamy, G. Kang, J. B. Kanner, S. Karki, M. Kasprzack, E. Katsavounidis, W. Katzman, S. Kaufer, T. Kaur, K. Kawabe, F. Kawazoe, F. Kéfélian, M. S. Kehl, D. Keitel, D. B. Kelley, W. Kells, R. Kennedy, D. G. Keppel, J. S. Key, A. Khalaidovski, F. Y. Khalili, I. Khan, S. Khan, Z. Khan, E. A. Khazanov, N. Kijbunchoo, C. Kim, J. Kim, K. Kim, Nam-Gyu Kim,

Namjun Kim, Y.-M. Kim, E. J. King, P. J. King, D. L. Kinzel, J. S. Kissel, L. Kleybolte, S. Klimenko, S. M. Koehlenbeck, K. Kokeyama, S. Koley, V. Kondrashov, A. Kontos, S. Koranda, M. Korobko, W. Z. Korth, I. Kowalska, D. B. Kozak, V. Kringel, B. Krishnan, A. Królak, C. Krueger, G. Kuehn, P. Kumar, R. Kumar, L. Kuo, A. Kutynia, P. Kwee, B. D. Lackey, M. Landry, J. Lange, B. Lantz, P. D. Lasky, A. Lazzarini, C. Lazzaro, P. Leaci, S. Leavey, E. O. Lebigot, C. H. Lee, H. K. Lee, H. M. Lee, K. Lee, A. Lenon, M. Leonardi, J. R. Leong, N. Leroy, N. Letendre, Y. Levin, B. M. Levine, T. G. F. Li, A. Libson, T. B. Littenberg, N. A. Lockerbie, J. Logue, A. L. Lombardi, L. T. London, J. E. Lord, M. Lorenzini, V. Loriette, M. Lormand, G. Losurdo, J. D. Lough, C. O. Lousto, G. Lovelace, H. Lück, A. P. Lundgren, J. Luo, R. Lynch, Y. Ma, T. MacDonald, B. Machenschalk, M. MacInnis, D. M. Macleod, F. Magaña Sandoval, R. M. Magee, M. Mageswaran, E. Majorana, I. Maksimovic, V. Malvezzi, N. Man, I. Mandel, V. Mandic, V. Mangano, G. L. Mansell, M. Manske, M. Mantovani, F. Marchesoni, F. Marion, S. Márka, Z. Márka, A. S. Markosyan, E. Maros, F. Martelli, L. Martellini, I. W. Martin, R. M. Martin, D. V. Martynov, J. N. Marx, K. Mason, A. Masserot, T. J. Massinger, M. Masso-Reid, F. Matichard, L. Matone, N. Mavalvala, N. Mazumder, G. Mazzolo, R. McCarthy, D. E. McClelland, S. McCormick, S. C. McGuire, G. McIntyre, J. McIver, D. J. McManus, S. T. McWilliams, D. Meacher, G. D. Meadors, J. Meidam, A. Melatos, G. Mendell, D. Mendoza-Gandara, R. A. Mercer, E. Merilh, M. Merzougui, S. Meshkov, C. Messenger, C. Messick, P. M. Meyers, F. Mezzani, H. Miao, C. Michel, H. Middleton, E. E. Mikhailov, L. Milano, J. Miller, M. Millhouse, Y. Minenkov, J. Ming, S. Mirshekari, C. Mishra, S. Mitra, V. P. Mitrofanov, G. Mitselmakher, R. Mittleman, A. Moggi, M. Mohan, S. R. P. Mohapatra, M. Montani, B. C. Moore, C. J. Moore, D. Moraru, G. Moreno, S. R. Morriss, K. Mossavi, B. Mours, C. M. Mow-Lowry, C. L. Mueller, G. Mueller, A. W. Muir, Arunava Mukherjee, D. Mukherjee, S. Mukherjee, N. Mukund, A. Mullavey, J. Munch, D. J. Murphy, P. G. Murray, A. Mytidis, I. Nardecchia, L. Naticchioni, R. K. Nayak, V. Necula, K. Nedkova, G. Nelemans, M. Neri, A. Neunzert, G. Newton, T. T. Nguyen, A. B. Nielsen, S. Nissanke, A. Nitz, F. Nocera, D. Nolting, M. E. N. Normandin, L. K. Nuttall, J. Oberling, E. Ochsner, J. O'Dell, E. Oelker, G. H. Ogin, J. J. Oh, S. H. Oh, F. Ohme, M. Oliver, P. Oppermann, Richard J. Oram, B. O'Reilly, R. O'Shaughnessy, C. D. Ott, D. J. Ottaway, R. S. Ottens, H. Overmier, B. J. Owen, A. Pai, S. A. Pai, J. R. Palamos, O. Palashov, C. Palomba, A. Pal-Singh, H. Pan, Y. Pan, C. Pankow, F. Pannarale, B. C. Pant, F. Paoletti, A. Paoli, M. A. Papa, H. R. Paris, W. Parker, D. Pascucci, A. Pasqualetti, R. Passaquieti, D. Passuello, B. Patricelli, Z. Patrick, B. L. Pearlstone, M. Pedraza, R. Pedurand, L. Pekowsky, A. Pele, S. Penn, A. Perreca, H. P. Pfeiffer, M. Phelps, O. Piccinni, M. Pichot, M. Pickenpack, F. Piergiovanni, V. Pierro, G. Pillant, L. Pinard, I. M. Pinto, M. Pitkin, J. H. Poeld, R. Poggiani, P. Popolizio, A. Post, J. Powell, J. Prasad, V. Predoi, S. S. Premachandra, T. Prestegard, L. R. Price, M. Prijatelj, M. Principe, S. Privitera, R. Prix, G. A. Prodi, L. Prokhorov, O. Puncken, M. Punturo, P. Puppo, M. Pürrer, H. Qi, J. Qin, V. Quetschke, E. A. Quintero, R. Quitzow-James, F. J. Raab, D. S. Rabeling, H. Radkins, P. Raffai, S. Raja, M. Rakhmanov, C. R. Ramet, P. Rapagnani, V. Raymond, M. Razzano, V. Re, J. Read, C. M. Reed, T. Regimbau, L. Rei, S. Reid, D. H. Reitze, H. Rew, S. D. Reyes, F. Ricci, K. Riles, N. A. Robertson, R. Robie, F. Robinet, A. Rocchi, L. Rolland, J. G. Rollins, V. J. Roma, J. D. Romano, R. Romano, G. Romanov, J. H. Romie, D. Rosińska, S. Rowan, A. Rüdiger, P. Ruggi, K. Ryan, S. Sachdev,

T. Sadecki, L. Sadeghian, L. Salconi, M. Saleem, F. Salemi, A. Samajdar, L. Sammut, L. M. Sampson, E. J. Sanchez, V. Sandberg, B. Sandeen, G. H. Sanders, J. R. Sanders, B. Sassolas, B. S. Sathyaprakash, P. R. Saulson, O. Sauter, R. L. Savage, A. Sawadsky, P. Schale, R. Schilling, J. Schmidt, P. Schmidt, R. Schnabel, R. M. S. Schofield, A. Schönbeck, E. Schreiber, D. Schuette, B. F. Schutz, J. Scott, S. M. Scott, D. Sellers, A. S. Sengupta, D. Sentenac, V. Sequino, A. Sergeev, G. Serna, Y. Setyawati, A. Sevigny, D. A. Shaddock, T. Shaffer, S. Shah, M. S. Shahriar, M. Shaltev, Z. Shao, B. Shapiro, P. Shawhan, A. Sheperd, D. H. Shoemaker, D. M. Shoemaker, K. Siellez, X. Siemens, D. Sigg, A. D. Silva, D. Simakov, A. Singer, L. P. Singer, A. Singh, R. Singh, A. Singhal, A. M. Sintes, B. J. J. Slagmolen, J. R. Smith, M. R. Smith, N. D. Smith, R. J. E. Smith, E. J. Son, B. Sorazu, F. Sorrentino, T. Souradeep, A. K. Srivastava, A. Staley, M. Steinke, J. Steinlechner, S. Steinlechner, D. Steinmeyer, B. C. Stephens, S. P. Stevenson, R. Stone, K. A. Strain, N. Straniero, G. Stratta, N. A. Strauss, S. Strigin, R. Sturani, A. L. Stuver, T. Z. Summerscales, L. Sun, P. J. Sutton, B. L. Swinkels, M. J. Szczepańczyk, M. Tacca, D. Talukder, D. B. Tanner, M. Tápai, S. P. Tarabrin, A. Taracchini, R. Taylor, T. Theeg, M. P. Thirugnanasambandam, E. G. Thomas, M. Thomas, P. Thomas, K. A. Thorne, K. S. Thorne, E. Thrane, S. Tiwari, V. Tiwari, K. V. Tokmakov, C. Tomlinson, M. Tonelli, C. V. Torres, C. I. Torrie, D. Töyrä, F. Travasso, G. Traylor, D. Trifirò, M. C. Tringali, L. Trozzo, M. Tse, M. Turconi, D. Tuyenbayev, D. Ugolini, C. S. Unnikrishnan, A. L. Urban, S. A. Usman, H. Vahlbruch, G. Vajente, G. Valdes, M. Vallisneri, N. van Bakel, M. van Beuzekom, J. F. J. van den Brand, C. Van Den Broeck, D. C. Vander-Hyde, L. van der Schaaf, J. V. van Heijningen, A. A. van Veggel, M. Vardaro, S. Vass, M. Vasúth, R. Vaulin, A. Vecchio, G. Vedovato, J. Veitch, P. J. Veitch, K. Venkateswara, D. Verkindt, F. Vetrano, A. Viceré, S. Vinciguerra, D. J. Vine, J.-Y. Vinet, S. Vitale, T. Vo, H. Vocca, C. Vorvick, D. Voss, W. D. Vousden, S. P. Vyatchanin, A. R. Wade, L. E. Wade, M. Wade, S. J. Waldman, M. Walker, L. Wallace, S. Walsh, G. Wang, H. Wang, M. Wang, X. Wang, Y. Wang, H. Ward, R. L. Ward, J. Warner, M. Was, B. Weaver, L.-W. Wei, M. Weinert, A. J. Weinstein, R. Weiss, T. Welborn, L. Wen, P. Weßels, T. Westphal, K. Wette, J. T. Whelan, S. E. Whitcomb, D. J. White, B. F. Whiting, K. Wiesner, C. Wilkinson, P. A. Willems, L. Williams, R. D. Williams, A. R. Williamson, J. L. Willis, B. Willke, M. H. Wimmer, L. Winkelmann, W. Winkler, C. C. Wipf, A. G. Wiseman, H. Wittel, G. Woan, J. Worden, J. L. Wright, G. Wu, J. Yablon, I. Yakushin, W. Yam, H. Yamamoto, C. C. Yancey, M. J. Yap, H. Yu, M. Yvert, A. Zadrożny, L. Zangrando, M. Zanolin, J.-P. Zendri, M. Zevin, F. Zhang, L. Zhang, M. Zhang, Y. Zhang, C. Zhao, M. Zhou, Z. Zhou, X. J. Zhu, M. E. Zucker, S. E. Zuraw, and J. Zweizig. Observation of gravitational waves from a binary black hole merger. *Phys. Rev. Lett.*, 116:061102, Feb 2016.

[3] J.S. Bendat and A.G. Piersol. *Random Data: Analysis and Measurement Procedures*. Wiley Series in Probability and Statistics. Wiley, 2011.

[4] Eric D. Black. An introduction to pound–drever–hall laser frequency stabilization. *American Journal of Physics*, 69(1):79–87, 2001.

[5] E Goetz, P Kalmus, S Erickson, R L Savage, G Gonzalez, K Kawabe, M Landry, S Marka, B O'Reilly, K Riles, D Sigg, and P Willems. Precise calibration of LIGO test mass ac-

tuators using photon radiation pressure. *Classical and Quantum Gravity*, 26(24):245011, nov 2009.

[6] Anchal Gupta, Francisco Salces-Carcoba, Yehonathan Drori, and Rana Adhikari. 0.1% uncertainty multicolor calibration scheme for gravitational wave detectors. In *APS April Meeting Abstracts*, volume 2022 of *APS Meeting Abstracts*, page F01.070, January 2022.

[7] Kiwamu Izumi, Koji Arai, Bryan Barr, Joseph Betzwieser, Aidan Brooks, Katrin Dahl, Suresh Doravari, Jennifer C. Driggers, W. Zach Korth, Haixing Miao, Jameson Rollins, Stephen Vass, David Yeaton-Massey, and Rana X. Adhikari. Multicolor cavity metrology. *Journal of the Optical Society of America A*, 29(10):2092, sep 2012.

[8] Adam J. Mullavey, Bram J. J. Slagmolen, John Miller, Matthew Evans, Peter Fritschel, Daniel Sigg, Sam J. Waldman, Daniel A. Shaddock, and David E. McClelland. Arm-length stabilisation for interferometric gravitational-wave detectors using frequency-doubled auxiliary lasers. *Opt. Express*, 20(1):81–89, Jan 2012.